DOI: 10.47743/achi-2023-2-0014 *ACTA CHEMICA IASI*, 31_2, 221-250 (2023)

SYNTHESIS, COMPLEXATION, SPECTRAL AND ANTIBACTERIAL STUDY OF (((4-METHOXYBENZOTHIAZOL-2-YL)IMINO)-6-BROMO) NAPHTHALEN-2-OL LIGAND

Fawzi Yahya Wadday[a*], Sahar Aqeel Hussain[b]

[a]*Department of Chemistry, Faculty of Science, Kufa University, Al-Najaf-Iraq*
[b]*Department of Pharmaceutical Chemistry, Faculty of Pharmacy, University of Kufa, Al-Najaf, Iraq*

Abstract: A new substituted 4-Methoxy-2-aminobenzothiazole ligand containing an azomethine (-N=CH-) group, (((4-methoxybenzothiazol-2-yl)imino)6-bromo) naphthalene-2-ol (MTIBN) was synthesized by the reaction of 2-amino-4-methoxybenzothiazole with 6-bromo-2-hydroxy-1-naphthaldehyde in absolute ethanolic solution. The ligand (MTIBN) has been identified by using ^{1}H, ^{13}C-NMR spectroscopy, mass spectroscopy, and Micro Elemental Analysis (C.H.N.S), as well as UV-Visible and (FT-IR). Mononuclear complexes of a bidentate hydroxy-azomethine ligand were synthesized by reaction with nickel(II), cobalt(II), copper(II) and palladium chloride salts. The complexes, $[Co(MTIBN)(H_2O)_2]$, $[Ni(MTIBN)(H_2O)_2]$, $[Cu(MTIBN)(H_2O)_2]$ and [Pd(MTIBN)] were characterized by elemental analysis, FT-IR, UV-Visible, atomic absorption, magnetic susceptibility, and C.H.N.S. The mononuclear Co(II), Ni(II), Cu(II), and Pd(II) complexes of the ligand have a metal: ligand ratio of 1:2 and the ligand coordinates through the O and N atoms. The molar conductivities in the DMSO solution indicate the non-electrolytic nature of the metal chelates. The antimicrobial activities of the ligand and its metal complexes were tested against *Staphylococcus aureus* and *Escherichia coli* human pathogenic. The results show that the synthesized new compounds had effective antimicrobial activities.

Keywords: Complexation, Spectral, Mass spectroscopy, Antimicrobial activity, Azomethine**.**

Introduction

Recent years have seen a lot of research on the new chemical compound class, Schiff bases; these compounds have azomethine (-N=C-)

* Fawzi Yahya Wadday, *e-mail*: fawzi.almwuashi@uokufa.edu.iq

that has been extensively studied.[1] The nitrogen atom in the azomethine group possesses electronic properties that allow it to form specific and flexible chemical bonds with metal ions; this is due to the presence of two unpaired electrons on the nitrogen atom. Low-valent metals are stabilized by them when they are in low oxidation states. A phenyl ring fused thiazole ring structure, 2-aminobenzothiazole has a molecular formula of $C_7H_6N_2S$.[2] A wide spectrum of biological activities is associated with several 2-Aminobenzothiazole derivatives in the medicinal and pharmaceutical chemistry fields.[3] Due to their multi-coordination modes, thiazole derivatives are particularly important for pharmaceutical applications and medicinal purposes, they have been found to have many health benefits, including fighting against harmful microorganisms, preventing degenerative diseases, reducing inflammation, fighting tumors, lowering high blood pressure, and even killing cancer cells. As a result, many medications that contain this molecule are available on the market.[4,5] The inorganic chemistry branch was established by scientists in the nineteenth century through the study and creation of numerous bonds that confine atoms in a state conducive to forming stable coordination bonds with metallic and other elements. Since coordination compounds are important in many areas, including the analytical aspect of mineral extraction, they are interest to many researchers and academics.[6] As organic ligands, Schiff base forms complexes with many metals. This lone pair aids in creating monodentate complexes, while adding other groups, such as OH, NH_2 and SH, may result in the formation of bidentate chelates.[7] Their bright colors, antioxidant properties, and corrosion resistance made azomethine ligands and complexes useful in spectroscopy.[8] It is fascinating to study the complexes formed between Schiff base and its derivatives with metal ions in chemistry, biology, and industrial biology. With every new coordination complex, a new understanding of the coordination

process emerges, a new challenge is presented, and new scientific knowledge is gained in various useful areas, making coordination compounds an inexhaustible aid in all new synthetic chemistry. As a result, coordination compound chemistry has grown into a world of its own and includes a wide range of topics. Also among the most important coordination compounds are Schiff compounds, which have an important role in all scientific fields.[9] This work includes synthesizing a new Schiff base ligand via treated 4-methoxy-2-aminobenzothiazole and 6-bromo-2-hydroxy-1-naphthaldehyde in glacial acetic acid. In view of the importance of coordination complexes, four coordination complexes have been prepared, characterized and antibacterial studies have been conducted. The complexes were synthesized by combining 2-amino-4-methylbenzothiazole and 6-bromo-2-hydroxy-1-naphthaldehyde with metal dichloride salt of Co, Ni, Cu, and Pd.

Experimental section

Instrumentation

A Thermometer Stuart apparatus, model SMP30 LTD.UK, was used to determine melting points for prepared compounds. The WTW 720 digital conductivity meter was used to test the electrical conductivity for complexes at (25 ^{o}C) for 10^{-3} mol·L^{-1} solutions for materials in dimethylsulfoxide (DMSO). Shimadzu UV-Visible spectrophotometer Ser. No. (206-24101-93) was used to record electronic spectra in ethanol solvent within 200-1100 nm wavelength using quartz cell of (1.0) cm length, Shimadzu spectrophotometer Ser. No. (604-8511) was used to `record FT-IR spectra in the region of 4000-400 cm^{-1} in KBr. Bruker DRX (500-MHz, 125-MHz) spectrometer was used to record ^{1}H and ^{13}C NMR spectra in DMSO-d6 and Bruner DRX, chemical shift are measured in parts per million (ppm) relative to the internal Me_4Si standard. An Agilent mass spectrometer 5975 quadrupole analyzer was

used to measure the mass spectrum for the ligand. Elemental microanalysis was done on the ligand and its complexes with the Euro Vectro-3000 A. Analytic Jena (VARIO 6, AG) atomic absorption Spectrophotometer evaluated the metal content of the complexes using atomic absorption technology Limited Liability Company (LLC) for management (UK), Magnetic susceptibility of prepared complexes was determined at room temperature by used the Faraday's method, Auto Magnetic Susceptibility Balance Model -MSB MKI. Thin Layer Chromatography (TLC) was carried out on Al plates covered with Fluka silica gel and iodine has been used for detection. The materials and the compound solutions used in the biological study were Sterilized by using an Autoclave, Gallen Kamp, and the cultivated bacteria dishes were incubated by using Memmert Incubator, 854 Schwach.

Materials

All chemicals used were of highest purity. B.D.H., Fluka, and Merck were used without further purification. Metal chloride "$CoCl_2 \cdot 6H_2O$, $NiCl_2 \cdot 6H_2O$, $CuCl_2 \cdot 2H_2O$, $PdCl_2$", 2-amino-4-methoxybenzothiazole, 6-bromo-2-hydroxy-1-naphthaldehyde, glacial acetic acid, Mueller Hinton agar, absolute ethanol, benzene, dimethylsulfoxide, dimethylformamide, methanol, hexane, dimethyl ether, acetone and distilled water.

Synthesis of the Ligand (MTIBN)

A 200 mL flask containing 0.18 gram (0.001 mol) of 2-amino-4-methoxybenzothiazole powder along with 15 mL of absolute ethanol. Using (0.251 g, 0.001 mol) 6-bromo-2-hydroxy-1-naphthaldehyde in ethanol (15 mL) solution and 3 drops of glacial acetic acid was added and refluxed for four hours. A pale brown precipitate mass formed, and which was subsequently separated from the solution.[10] Recrystallizing the resulting mass

in hot ethanol yielded mass crystalline substance with a melting point of (147 °C) and a yield of 79 %. R_f (0.53) in a solvent solution of benzene and ethanol (7:3) (v/v). The Scheme 1 below describes the reaction.

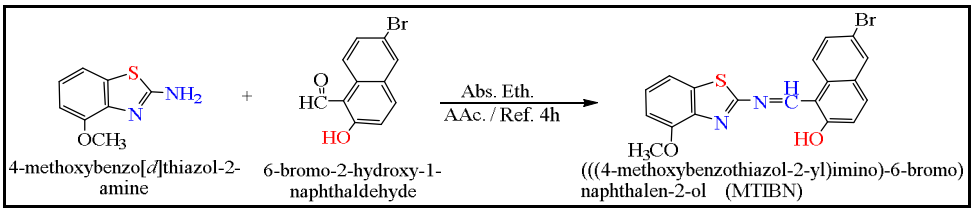

Scheme 1. Synthesis route of a new ligand MTIBN.

Preparing the standard solution

Standard solutions of the metal salts and ligand as stock solutions were prepared by dissolving the appropriate weight at a concentration ($1x10^{-3}$ M). (0.001 mol) of each the following salts $CoCl_2·6H_2O$, $NiCl_2·6H_2O$, $CuCl_2·2H_2O$, and $Pd(CH_3CN)_2Cl_2$ in the (100 mL) ethanol solvent. From those standard solutions above were prepared several concentrations at ($1×10^{-4}$ – $5.5×10^{-4}$) M.

The stoichiometry of the ligand

To determine the M:L ratio, the data of various ligand-metal solutions mixtures was measured using the mole ratio method. The experimental procedure followed the outlined below.

Synthesis of metal complexes

A solution of 0.0001 mol of metal chloride (0.0238 g $CoCl_2·6H_2O$, 0.0237 g $NiCl_2·6H_2O$, 0.0170 g $CuCl_2·2H_2O$, 0.0223 g $PdCl_2$) in 10 mL ethanol was added to a mixture of ligand (0.0002 mol, 0.0823 g) in 10 mL ethanol. After heating the solutions for an hour, the complexes were gently precipitated by evaporation then filtered off, washed with a mixture of (5:5)

water and ethanol. Scheme 2 describes the process of preparation and recrystallizing the complexes from heated ethanol. Methanol, ethanol dimethylformamide, and dimethylsulfoxide are all effective and perfect solvents for dissolving isolated complexes which are colorful solid compounds that are stable in air but insoluble in normal organic solvents particularly hexane, diethyl ether, and acetone. Table 1 describes the quantity, yield percentage and Retention factor data for MTIBN and its complexes in the hexane–ethanol (3:7) (v/v) as an eluent.

Table 1. Yield percentage, mass quantity and Rf for MTIBN and its complexes.

Compound Formula	**Wt.(g) of (1 mol)**	**Yield %**	**R_f**
L=(MTIBN) ($C_{19}H_{13}N_2O_2SBr$)	411.99	79	0.53
$[Co(C_{38}H_{24}N_4O_4S_2Br_2)(H_2O)_2]$	919.53	77	0.5
$[Ni(C_{38}H_{24}N_4O_4S_2Br_2)(H_2O)_2]H_2O$	933.3	75	0.47
$[Cu(C_{38}H_{24}N_4O_4S_2Br_2)(H_2O)_2]$	924.14	81	0.48
$[Pd(C_{38}H_{24}N_4O_4S_2Br_2)(H_2O)_2]H_2O$	985.03	72	0.42

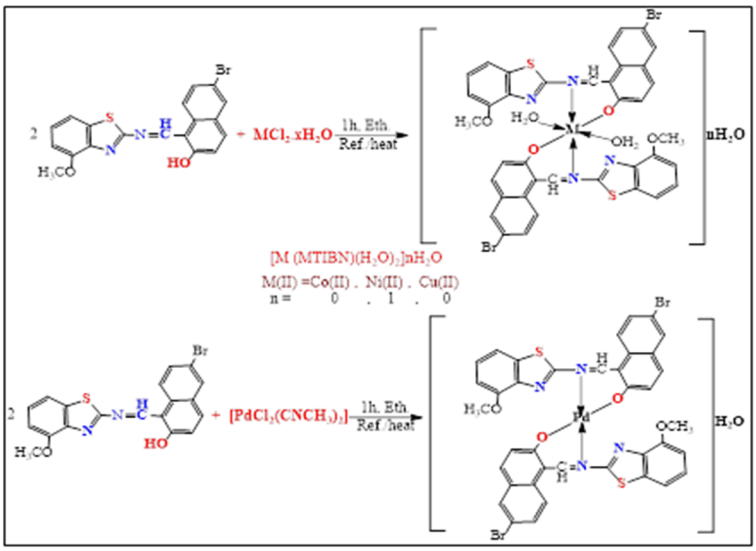

Scheme 2. Synthesis pathway of metals ion complexes with MTIBN.

Study of the solubility of ligand and its complexes

This study was conducted for the purpose of knowing the effect of the solvent on the solubility of the ligand and its metal compounds, the solubility of all prepared complexes was tested in different solvents and through this survey, a solubility of these compounds was investigated with various organic solvents that have different polarities, including ethanol, methanol, dimethylsulfoxide and dimethylformamide, some of which are used to conduct the practical experiments.

Antimicrobial Study

The agar-well diffusion technique was applied in testing all of the recently synthesized ligand and complexes against *Staphylococcus aureus* which are Gram (+) and *E-coli* and, Gram (-). All of the compounds were found to be effective against the bacteria.[11] Muller Hinton Agar was used as the medium for the cultivation of the microorganisms to be tested.[12] DMSO, with a purity of 99.9% is utilized as a solvent in preparing chemical solutions for biological studies. It is chosen as a solvent due to its unique characteristics, such as being a polar aprotic solvent, non-toxic, relatively inert, non-dissociating, and weakly acidic, which prevents it from having a high pH value, where the prepared solutions' acidity function was 6.8 in this solvent. The sensitivity test was carried out by preparing sterile Muller Hinton agar from dissolving 38 g in 1 L distilled water and carefully transferring it into sterile Petri dishes to an appreciable amount. The media was allowed to cool and solidify at room temperature. The agar plates were surface inoculated uniformly from the broth culture of the tested microorganisms (using a glass spreader) 0.1 mL of bacteria inoculums was done on the surface

of dried Muller Hinton agar. In the solidified medium, suitably spaced apart, four holes were made (6 mm diameter) and filled with 10 µL of the synthesized compounds that were dissolved in dimethyl sulfoxide (Using the relationship between molar concentration and ppm concentration, three solutions were made with diluted concentrations for each constituent from the stock solution, which had a concentration of 0.001 molar). The dilutions were prepared at the required quantities of 100, 200 and 400 $\mu g.mL^{-1}$ concentrations. To ensure that the solvent did not affect bacterial growth, control test was also performed containing a hole loaded with only DMSO at the same dilution used in our experiment. The Petri dishes were marked to indicate bacteria and the positions of the wells of different test concentrations for both the ligand and complexes. These petri dishes were incubated at (37 ^{o}C) for (24 hrs.). After that, the inhibition zones caused by the various compounds on the bacteria were measured by the use of the millimeter ruler.

Results and Discussion

Physical characteristics and elemental examination

Ligand (MTIBN) is pale brown in color. Different colored crystals are produced when this ligand reacts with the metal ions that are used. All compounds are stable in air-and insoluble in water but soluble in most organic solvents like ethanol, methanol, diethyl ether, acetone, dimethyl sulfoxide, carbon tetrachloride. Table 2 shows physical features and results of elemental analysis (C, H, N and S) examination and the organized compounds' metal substances. With planned magnitudes, the investigating data is satisfactory.

NMR Spectra for the MTIBN ligand

^{1}H-NMR spectrum Figure 1 of (MTIBN) in DMSO-d6 showed numerous signals; a naphthol-OH low signal strength was seen at

δ 11.09 ppm (s, 1H), while the signal at (δ= 8.74) ppm duo to (H-C=N) azomethine proton.[13] The aromatic protons were appeared at (δ= 8.46-7.06) and (7.42-6.50) ppm due to naphthol and benzothiazole rings protons respectively.[14] The signal at (δ= 3.81 ppm) assigned to methyl proton (CH_3-O) that attached with benzothiazole ring.[15]

Table 2. Physical properties and analytical statistics of MTIBN and its complexes.

Empirical formula	Color	M.P °C	Element Analysis Found (calctd.) %.				Found (calctd.) Metal %
			C	H	N	S	
MTIBN = $C_{19}H_{13}N_2O_2SBr$	Pale brown	147	55.22 (55.06)	3.17 (3.11)	6.78 (6.81)	7.76 (7.74)	——
$[Co(C_{38}H_{24}N_4O_4S_2Br_2)(H_2O)_2]$	Brown	171	49.63 (48.61)	3.06 (3.11)	6.09 (5.99)	6.97 (6.90)	6.40 (6.33)
$[Ni(C_{38}H_{24}N_4O_4S_2Br_2)(H_2O)_2]H_2O$	Deep green	165	48.69 (48.59)	3.22 (3.26)	5.97 (5.99)	6.84 (6.81)	6.26 (6.21)
$[Cu(C_{38}H_{24}N_4O_4S_2Br_2)(H_2O)_2]$	Pale green	189 °D	49.38 (49.41)	3.05 (3.12)	6.06 (6.11)	6.93 (6.97)	6.87 (6.94)
$[Pd(C_{38}H_{24}N_4O_4S_2Br_2)]H_2O$	Deep orange	176	48.09 (48.03)	2.76 (2.78)	5.90 (5.94)	6.75 (6.73)	11.21 (11.13)

°D= Decomposition

The ^{13}C-NMR spectrum in Figure 2 exhibited many chemical shifts, there is a thiazole ring (C7=N) peak at δ(176.35 ppm) [13]. The chemical shifts appeared at δ(164.85 ppm) assigned to the (C14=C15-OH) and (C2=N) carbon atoms of naphthol and azomethine respectively.[14] The chemical shifts at δ(154.35, 146.85, 132.29 ppm) are responsible for the (C11, C55, C4) in benzothiazole aromatic rings carbon atoms.[15] The shift appeared at δ(131.97 ppm) duo to (C12) carbon, while the shift at δ(128.78 ppm) attributed to (C20, C18) atoms, whereas the peak at (123.02 ppm) assigned to (C16) and the peak appeared at (118.13 ppm) duo to (C21 and C17) atoms, furthermore the peak at (112.91 ppm) was assigned to (C15 and C9) atoms. The chemical shifts appeared at δ(107.49 and 105.57 ppm) were assigned to

(C19 and C8) in contrast the shift at (100.81 ppm) due to (C13 and C10) benzene and naphthol rings carbons atoms, while the chemical shifts appeared at δ(55.66 ppm) was assigned to (C25) methoxy moiety carbon atom which appeared split in peak due to the coupling between a carbon atom and protons attached to it, where The carbon and protons undergo spin-spin coupling.[16]

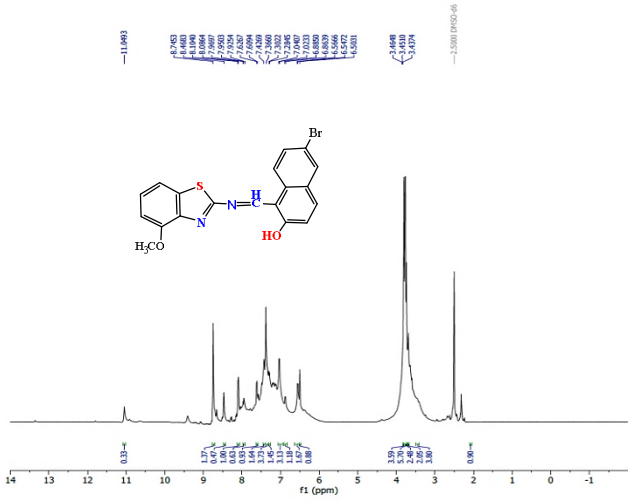

Figure 1. ^{1}H-NMR spectrum of MTIBN.

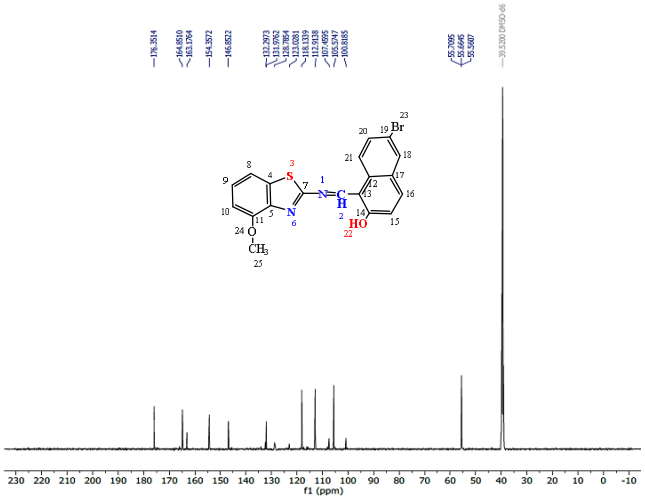

Figure 2. ^{13}C-NMR spectrum of MTIBN.

Mass spectrum for MTIBN

It was discovered that the molecular ion top at (m/z^+= 411.2) in the ligand's mass spectrum Figure 3 corresponded to $[C_{19}H_{22}N_2O_8]^+$.[17] Scheme 3 and Table 3 summarizes the other pieces and their relative abundance.

Table 3. Mass spectral data of MTIBN.

Fragments m/z^+	**Formula weight $g.mol^{-1}$**	**Relative abundance%**
$[C_{19}H_{13}N_2O_2SBr]^+$	411.2	8
$[C_{18}H_{10}BrN_2OS]^+$	380.1	15
$[C_{10}H_6BrO]^+$	220.1	21
$[C_8H_4N_2S]^{\bullet+}$	160.1	52
$[C_7H_4N_S]^+$	134	36
$[C_9H_6]^{\bullet+}$	114.1	100
$[C_6H_4]^{\bullet+}$	76	80

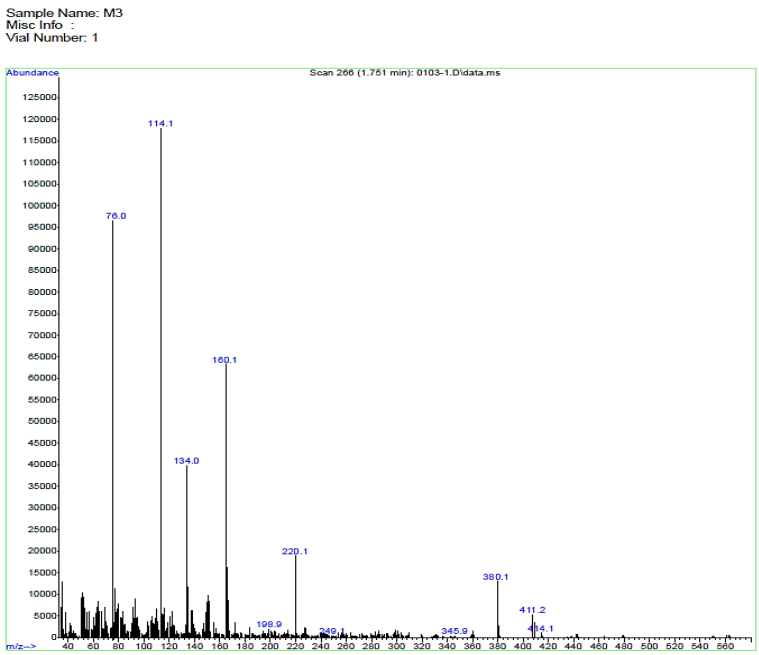

Figure 3. Mass spectrum of MTIBN.

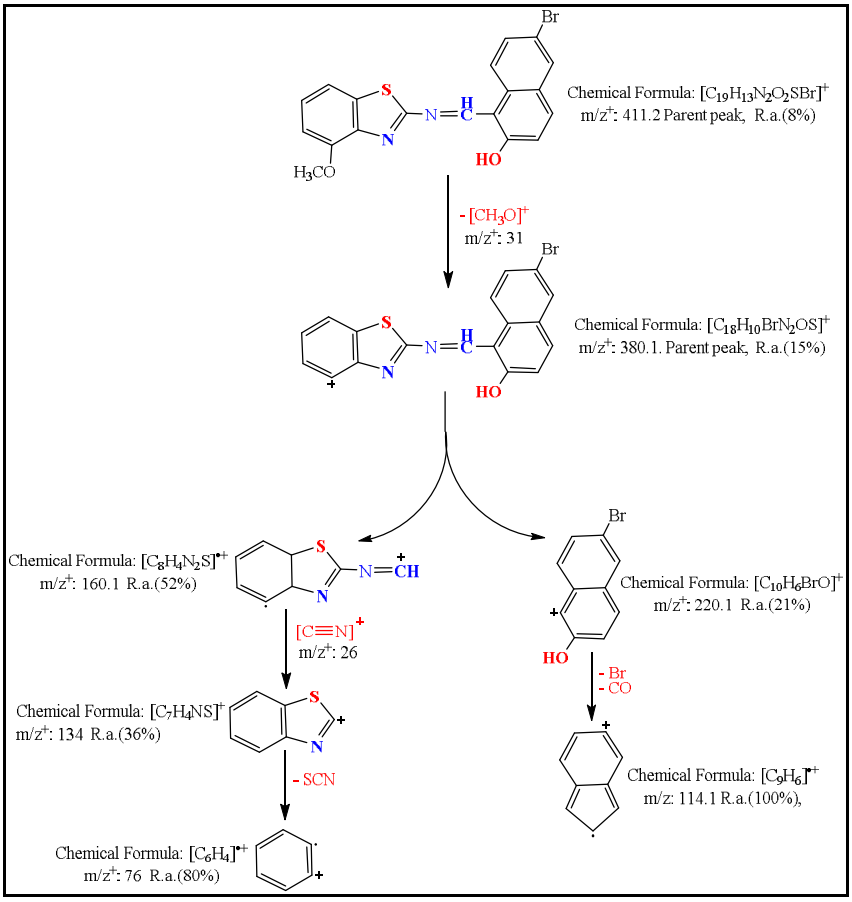

Scheme 3. The fragmentation of MTIBN.

Infrared spectra of MTIBN and its complexes

The FTIR spectra of the complexes were compared with that of the free ligand in order to determine the coordination sites involved in chelation and track changes that occur in some of them, which means the position of some instructor bands in the complexes spectra was expected to change from the free ligand spectrum due to the chelation.

A comparison of MTIBN spectrum Figures 4 with its metal complexes Figures 5 to 8. The frequency of the essential wide band at 3338 cm^{-1}, which attributed to the ν(O-H) stretching in the ligand, did not appear for any

complexes due to the loss of proton and sharing in coordination.[18] A band that was produced at 1548 cm^{-1} and was ascribed to the (C=N) stretching vibration of azomethine altered in shape and moved to a lower frequency in all complexes in the range of 1554-1529 cm^{-1}, these differences are considered a good indicator for coordination of the metal ions with nitrogen atom of azomethine group.[19,20] Broad bands at 3395, 3401 and 3382 cm^{-1} due to (O-H) stretching and bands at 860, 862 and 865 cm^{-1} in "Co(II), Ni(II) and Cu" complexes attributable to water coordination were found in all complexes except palladium complex.[21] The band at 1600 cm^{-1} in ligand spectrum assigned to υ(C=N) stretching vibration in benzothiazole ring this this band stretching was a very slight frequencies change in complexes spectra when it's compared with that band shape and energy in the free ligand spectrum, that means no involvement of (C=N) group in coordination.[20,21] The mediate bands which appeared ligand spectrum at 1219 and 1028 cm^{-1} duo to (C-N) and (C-S) groups in benzothiazole stretching vibration respectively, these bands stretching was a very slight frequencies change in complexes spectra drawing attention to the fact that they are not sharing in coordination.[21] New bands appeared in the spectra of all metal complexes that were not present in the ligand spectrum in the low-frequency at range 483-465 cm^{-1} and 446-431 cm^{-1} refers to (M-N) and (M-O) stretching vibration, respectively allocated to atoms that the ligands contributed with the metal ions in the complexes.[22] These observations in spectra of free ligand and its complexes indicated that the metal ions coordinate with ligand via (N, O) of azomethine, hydroxyl behaving bidentate toward metal ions in addition to (O) atoms of water as aqua ligand.[23] Table 4 summarizes the major IR bands and their potential assignments.

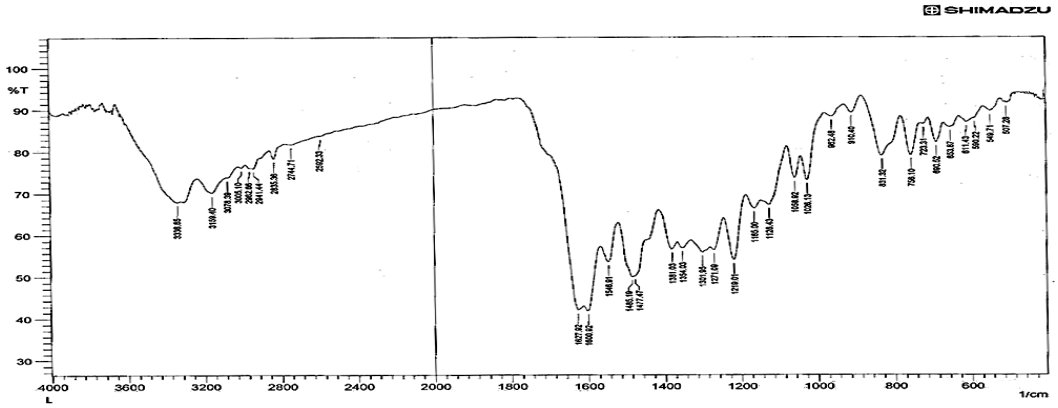

Figure 4. FT-IR spectrum of MTIBN.

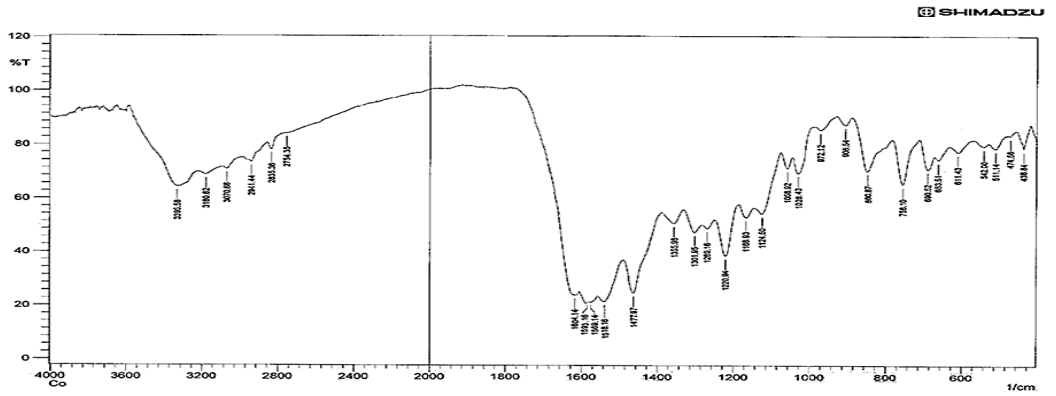

Figure 5. FTIR spectrum of Co(II) complex with MTIBN.

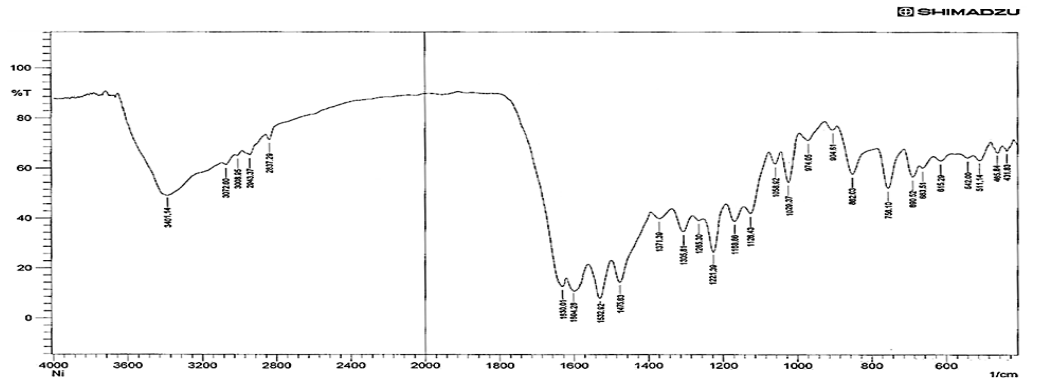

Figure 6. FTIR spectrum of Ni(II) complex with MTIBN.

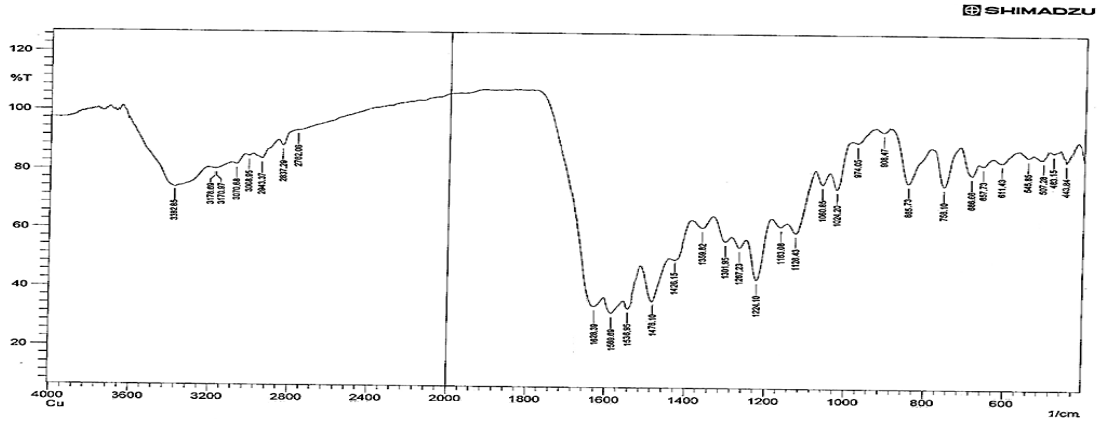

Figure 7. FTIR spectrum of Cu(II) complex with MTIBN.

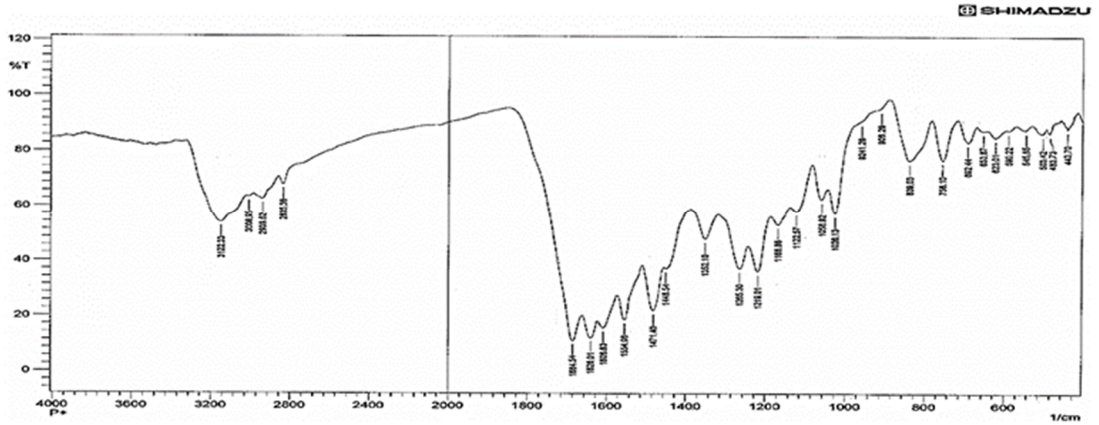

Figure 8. FTIR spectrum of Pd(II) complex with MTIBN.

Table 4. Characteristic FT-IR absorption bands of MTIBN and its complexes.

Compound	υO-H and Coord.Hydrate	υC=N benzothiazole	υC=N azomethine	υC-N	υC-S	δH_2O aqua	υM-N	υM-O
L= MTIBN	3338	1600	1548	1219	1026	-	-	-
L-Co	3395	1593	1537	1220	1028	860	474	438
L-Ni	3401	1604	1529	1221	1029	862	465	431
L-Cu	3382	1596	1536	1224	1024	865	471	446
L-Pd	-	1605	1554	1219	1022	-	483	443

Electronic spectra

The transition metal complexes prepared are colored and their colors are different from the transition metal salts and the ligand. Complexes of ligand with metal ions caused either bathochromic or hypsochromic shifts of ligand peaks. The intensities and positions of newly observed peaks related to (d→d) transition mainly depend on oxidation numbers and the position of metal ions in the periodic table and the stereochemistry of complexes.[21,22] The electronic spectra of the metal complexes Figures (10-13) in ethanol solution showed the bands corresponding to the intraligand π→π*and n→π* transitions shifted to lower energy, this observation in the metal complexes is relative to the free ligand have been attributed to complexation. The most significant alterations that took place in the complex spectra relative to the ligand spectrum resulting from the (d→d) transitions in the metal ions complexes can be summarized as follows. UV-Vis. spectrum of MTIBN revealed three absorptions as shown in Figure 9 at (228 nm, 43859.6 cm^{-1}) and the other at 273 nm, 36630 cm^{-1}) due to the $\pi-\pi^*$, and one at (415 nm, 24096.3 cm^{-1}) attributable to the $n-\pi^*$ transition.[21] Three bands can be seen in Figure 10 visible part of the Ni(II) complex's spectrum at (505 nm, 19801.9 cm^{-1}) $^3A_2g\rightarrow{}^3T_1g_{(P)}$ (υ_3), (712 nm, 14044.9 cm^{-1}) $^3A_2g\rightarrow{}^3T_1g_{(F)}$ (υ_2), the final one at (955 nm, 10471.2 cm^{-1}) $^3A_2g\rightarrow{}^3T_2g_{(F)}$, ($\upsilon_1$). On the Tanaba-Sugano diagram, the ratio of υ_2/υ_1 1.34, was used for the d^8 octahedral complexes, $B_{complex}$ (691.8), and β (0.65).[21] Two bands that emerged in Figure 11 at (680 nm, 14705.8 cm^{-1}) and (563 nm, 17761.9 cm^{-1}) in electronic spectrum for the Co-complex in ethanol solution were ascribed to the $^4T_1g\rightarrow{}^4A_2g$ (υ_2) and $^4T_1g\rightarrow{}^4T_1g_{(p)}$ (υ_3) transitions of octahedral geometry.[21,22] Using the diagram of Tanaba-Sugano for the d^7 arrangement of octahedral geometry, the $B_{complex}$ (605.63) value as well as the position of υ_1

(9627.3 cm^{-1}) were computed using the ratio of (υ_3)/(υ_2) (1.2).[23] The covalent nature is shown by the value of β (0.57). Broadband at (756 nm, 13227.5 cm^{-1}) in the Cu(II) complex spectrum Figure 12, was due to the $^2Eg \rightarrow {}^2T_2g$ transition, which is related to the distortion of the octahedral shape.[24] A band of high intensity in Figure 13, was observed at (512 nm, 19531.2 cm^{-1}) in the Pd(II) spectrum was ascribed to ($^1A_1g \rightarrow {}^1B_1g$), whereas the new at (589 nm, 16977.9) associated with the electronic transition type $^1A_1g \rightarrow {}^1A_2g$ in a square planar structure.[25] The electronic absorption bands are listed in Table 5.

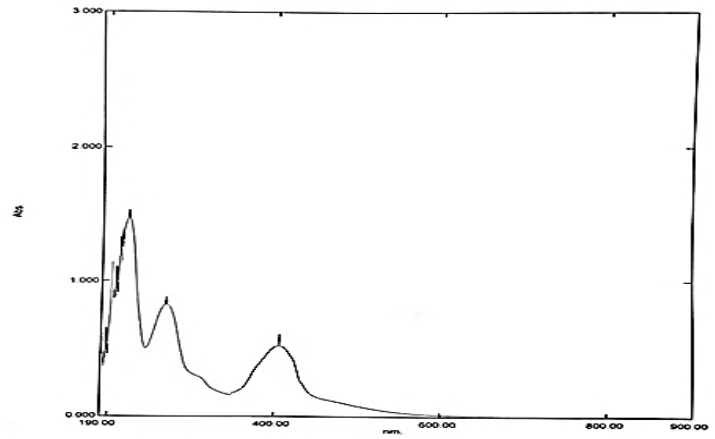

Figure 9. Electronic spectrum of MTIBN.

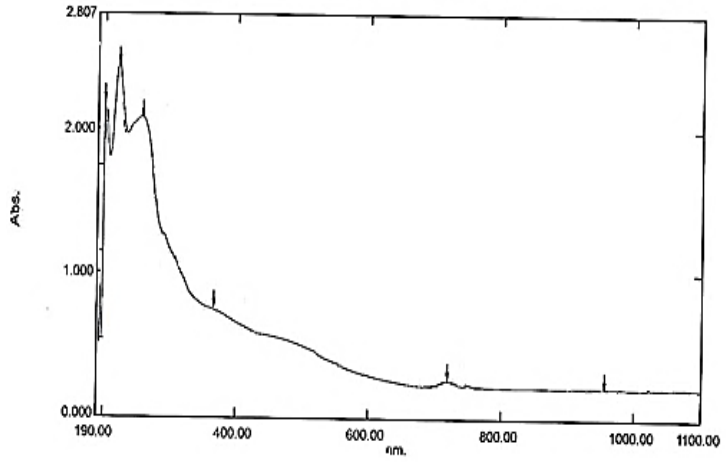

Figure 10. Electronic spectrum of MTIBN-Ni(II).

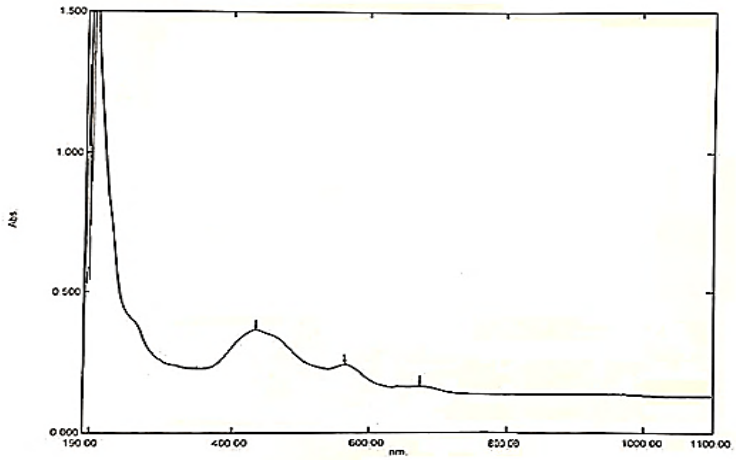

Figure 11. Electronic spectrum of MTIBN-Co(II).

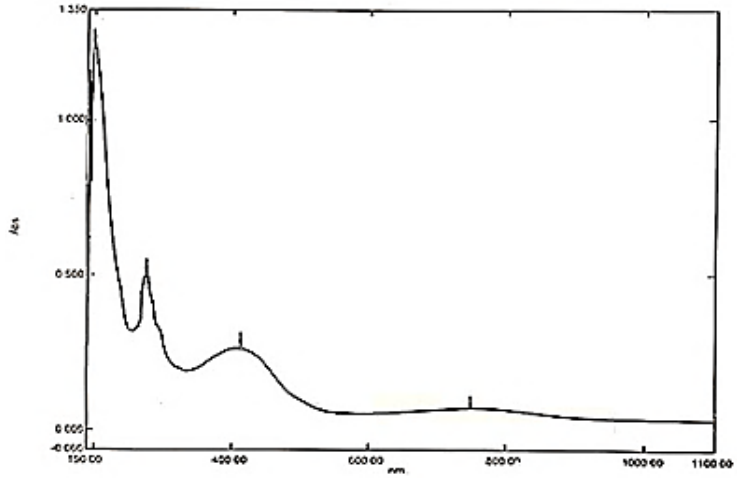

Figure 12. Electronic spectrum of MTIBN-Cu(II).

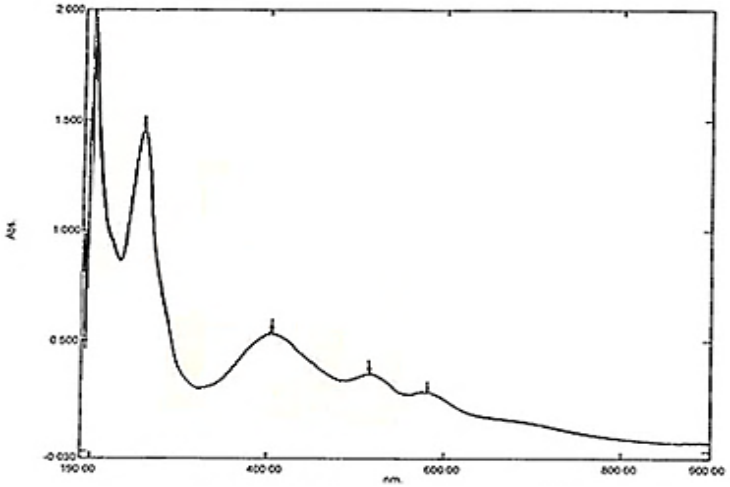

Figure 13. Electronic spectrum of MTIBN-Pd(II).

Table 5. Electronic spectra of MTIBN and its metal complexes, Racah B' and nephelauxetic β parameters measurements.

Complex	Band position nm	Band position cm^{-1}	Assignments	B' cm^{-1}	β	Proposed Structure	Hybridization
L=MTIBN	228 273 415	43859.6 36630 24096.3	π→π* π→π* n→π*	-------	-----	-------	------
L-Co(II)	563 680	17761.9 14705.8	$^4T_1g_{(F)}\rightarrow{}^4T_1g_{(p)}$ $^4T_1g_{(F)}\rightarrow{}^4A_2g_{(F)}$	607.14	0.57	Octahedral Distorted	sp^3d^2
L-Ni(II)	505 712 955	19801.9 14044.9 10471.2	$^3A_2g\rightarrow{}^3T_1g_{(p)}$ $^3A_2g\rightarrow{}^3T_1g_{(F)}$ $^3A_2g\rightarrow{}^3T_2g_{(F)}$	694.7	0.67	Octahedral	sp^3d^2
L-Cu(II)	756	13227.5	$^2Eg\rightarrow{}^2T_2g$	–	–	Octahedral Distorted	sp^3d^2
L-Pd(II)	512 589	19531.2 16977.9	$(^1A_1g\rightarrow{}^1B_1g)$ $(^1A_1g\rightarrow{}^1A_2g)$	–	–	Square planar	dsp^2

Magnetic measurements

The effective magnetic moments (μeff B.M) of metal complexes were measured in the solid state by Faraday's method. The magnetic properties provide testing ground for oxidation state of the metal in complex therefore provide a way of counting the number of unpaired electrons. This should help in predicting the bonding nature between metal ions with the ligand as well as electronic structure and geometry of complexes. The magnetic susceptibility data for complexes were measured by obtaining the sensitivity value (Xg) for each complex at (298 K) by using the following relationship:[21]

$$\mu\,\text{eff} = 2.83\sqrt{(\text{XA}.\text{T})}\ \text{B}.\text{M}. \quad (1)$$

$$\text{Xm} = \text{Xg} \times \text{Mwt} \quad (2)$$

$$\text{XA} = \text{Xm} - \text{D} \quad (3)$$

where: T= Temperature (K);
XA= Atomic susceptibility;
Xg= Grams susceptibility;
D= Diamagnetic correction factor susceptibility.

The results obtained from Faraday's method were compared with those calculated from spin only (μs.o), and contribution orbitals (μS+L) magnetic moment values. Due to the inherent orbital angular momentum d^7 Co(II)-complex, there is always a high orbital contribution in the ground state, and the effective magnetic moment at ambient temperature was between (4.7 and 5.2 B.M.). The magnetic moment magnitude of the present complex, which was 4.91 B.M., this obtained practical magnetism value is greater than the theoretical value computed for three individual electrons in orbital d^7, which value is equal to 3.88 BM. This is because the cobalt complex also exhibits a magnetic moment due to the contribution of the orbital moment in addition to the magnetic moment due to the electronic spin, where the magnetic moment coming from the orbital spin contribution supports the spin electronic magnetic moment, and the overall practical magnetism value calculated becomes greater than the theoretical value, suggested that the Co(II) complex in its high-spin form has the structure of an octahedron.[21,22] The orbital contribution magnitude is what determines the greater range of values of magnetic moment (2.9-3.4 B.M.) for the complex of d^8 a high-spin Ni(II). The magnetic moment obtained in this investigation, 3.06, was in the expected range like octahedral Ni(II) ions.[21,22] The Cu(II) complex magnetic moment was 1.81 B.M., and it was rather near the spin value expected for the d^9 (one unpaired electron) at 1.73 B.M. As a result, the Cu(II) complex has the structure of an octahedron.[26,27] Table 5 lists the magnetic moments that have been measured.

Conductivity measurements

Conductivity measurements are used to decide whether a complex is electrolytic or non-electrolytic. All complexes were dissolved in DMSO solvent ($1x10^{-3}$ M) concentration at room temperature, and they showed

molar conductivity values in the range (8.2 – 13.6 S.cm^2. mol^{-1}) indicating the (0:0) ratio electrolyte nature, this means that all the prepared complexes were non-electrolytes. These values for complexes were measured by obtaining the specific conductivity for each complex and applying the following equation:[21]

$$\Lambda m = 1000\,\mathrm{k} / \mathrm{C} \qquad (4)$$

where: Λm = Molar conductivity (S.cm^2.mol^{-1});

k = specific conductivity (S. cm^{-1});

C = concentration (mol /cm^3).

The complexes of Co(II), Cu(II), Ni(II) and Pd(II) had low conductivity at the above-mentioned solvent and a non-ionic structure.[21,27] Table 6 shows the conductivity values of all prepared complexes.

Table 6. Molar conductance and magnetic values of complexes.

Complexes formula	**μ_{eff}(B.M)**	**Λ_M (S.cm^2.mol^{-1})**
(MTIBN)-Co	4.91	8.2
(MTIBN)-Ni	3.06	12.5
(MTIBN)-Cu	1.81	10.1
(MTIBN)-Pd	Dia.	13.6

Proposed structures of prepared complexes

Based on the mentioned in the literature,[25,27] regarding the coordination sites available in the ligand and how it related to various metal ions through spectroscopic and analytical results that were obtained through the results of diagnostic measurements obtained from the molar ratio, elemental analysis, metals contents, magnetic measurements and the molar electrical conductivity measurements, as well as the results of the UV-Vis.

spectra and the (FT-IR) spectra indicated all the complexes have octahedral geometry except the palladium complex was a square planar, where the ligand behaved as bidentate coordination process through the oxygen of the hydroxyl group and nitrogen atoms of azomethine group bind the ligand to metal ions in addition to water as aqua resulting in six donated atoms to the metal ions with some exceptions in binding with platinum ion, Figure 14 drawn via the Chem. draw 2020 program that shown the geometrical of these compounds. There is a 1:2 mole ratio of M to L in these structures.

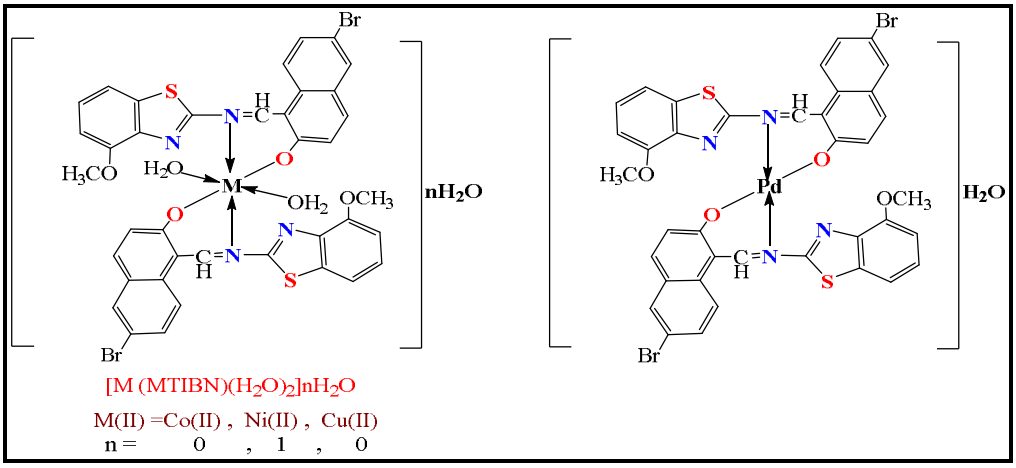

Figure 14. The suggested structural of metals ions complexes with MTIBN.

Antimicrobial activity

The *in-vitro* growth inhibitory MTIBN activities and their complexes on Gram (+) bacteria, such as *Staphylococcus aureus* and Gram (-) bacteria, namely *Escherichia coli*, were investigated using the spotted diffusion method. All of the substances exhibited a significant level of antibacterial activity when tested against the organisms in question with a high concentration of their solutions, at the same time, it did not show a significant inhibitory effect at two lower dilute concentrations. The Cu(II) complex with a high concentration showed higher antibacterial activity in *S. aureus*. There

was only a moderate amount of activity with the ligand and the complexes of Co(II), Ni(II) and Pd(II) at the same concentration. In contrast, the Cu(II) complex showed moderate antibacterial activity against *E. coli*, whereas the ligand and other complexes displayed slight activity. The *E. coli* bacteria exist as a single bacillus and have a thick shell that completely encases their cell. The high lipid content of this coating helps to prevent them from entering the cell, in contrast to the bacteria *S. aureus* which lack this characteristic, they will have a reduced ability to withstand the effects of chemical and antibiotic chemicals that penetrate the inside of the bacterial cell.[28] As a direct consequence of this, the chemical agents that were investigated had a more powerful inhibiting effect. Since the metal ions included inside metal complexes were lipophilic, metal complexes have a higher activity level than free ligands.[29] Through the process of chelation, the core metal atom becomes more lipophilic, which makes it possible for it to traverse the lipid layer of the cell membrane.[29,30] Variations in the antibacterial activity are caused by the properties of metal ions as well as the cell membranes of the microorganisms. According to overtone's theory chelation hypothesis, metal ion polarity is significantly reduced during chelation owing to ligand orbital overlaps and partial sharing of a metal ion's positive charge with donor groups, furthermore, the π -electron's delocalization is amplified across the whole chelate sphere, increasing the complex's lipophilicity. Chelation makes the core metal ion more lipophilic, allowing it to pass through the lipid layer of the cell membrane, the nature of metal ions and the cell membrane of microbes cause variances in antibiotic action. The antibacterial drugs' mode of action may be divided into four categories: Inhibition of cell wall function, cell membrane function, protein synthesis, and nucleic acid production.[31] The data are presented in Tables 7 and 8, while Figures 15 and 16 show the graphical depiction of the statistics.

Table 7. Inhibition area (mm) of the *S. aureus* sensitivity (zone inhibition) to the compounds.

Compound	Pathogenic bacteria ***S. aureus*, Gram(+)**	Concentration		
		100 ppm	**200 ppm**	**400 ppm**
Control (S)		6	6	6
DMSO				
Ligand (L)		6	6.1	10
L-Co		6	6	12
L-Ni		6	6.1	13.5
L-Cu		6	6.3	18
L-Pd		6	6.1	14

Table 8. Inhibition area (mm) of the *E. coli* sensitivity (zone inhibition) to the compounds.

Compound	Pathogenic bacteria ***E. coli*, Gram(-)**	Concentration		
		100 ppm	**200 ppm**	**400 ppm**
Control (S)		6	6	6
DMSO				
Ligand (L)		6	6	8
L-Co		6	6.1	9.5
L-Ni		6	6	10
L-Cu		6	6.2	13
L-Pd		6	6	10.5

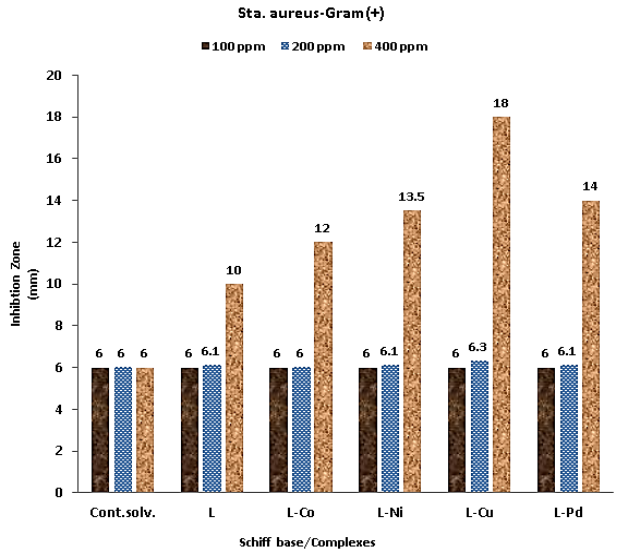

Figure 15. Statistical representation of antibacterial activity for Schiff base (MTIBN) and its complexes against (*Staphylococcus aureus*).

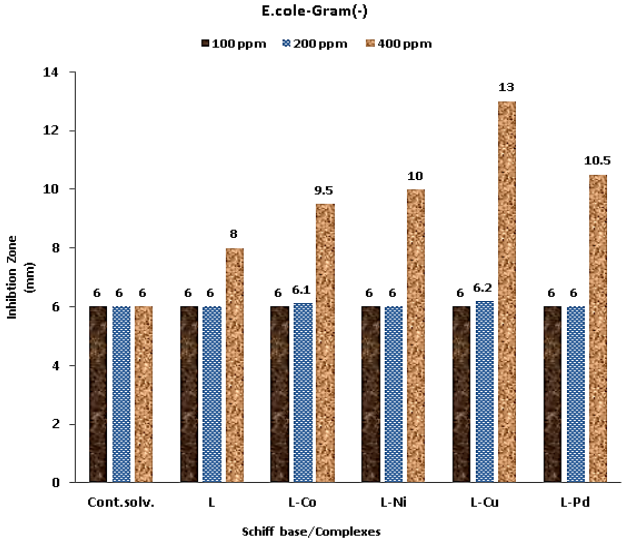

Figure 16. Statistical representation of antibacterial activity for Schiff base (MTIBN) and its complexes against (*Escherichia coli*).

Conclusion

Spectroscopic analyses such as elemental analysis, metal content, mass spectrum, ^{1}H, ^{13}C-NMR, FT-IR, and UV-Vis were used in this research to examine metal ions complexes of the new ligand, in addition to conductivity measurements and magnetic susceptibility testing support the

octahedral geometry of all complexes except the palladium complex was a square planar. There is a 1:2 mole ratio of M to L in these structures. The biological activity data of each chemical demonstrate its antibacterial properties at high concentration.

Acknowledgment

I would like to state my sincere thanks to the Department of Chemistry staff at the Faculty of Science, Kufa University.

References

1. Azam, M.; Al-Resayes, S. I.; Wabaidur, S. M.; Altaf, M.; Chaurasia, B.; Alam, M.; Shukla, S. N.; Gaur, P.; Albaqami, N. TM.; Islam, M. S. and Park, S. Synthesis, structural characterization and antimicrobial activity of Cu(II) and Fe(III) complexes incorporating Azo-Azomethine ligand. *Molecules* **2018**, *23*, 813.

2. Jordan, A. D; Vaidya, A. H.; Rosenthal, D. I; Dubinsky, B; Kordik, C. P; Sanfilippo, P. J; Wu, W.-N. and Reitz, A. B. Potential anxiolytic agents. part 4: novel orally-active N5-substituted pyrido [1,2-A] benzimidazoles with high GABA-A receptor affinity. *Bioorg. Med. Chem. Lett.* **2002**, *12*, 2381–2386.

3. Catalano, A.; Carocci, A.; Defrenza, I.; Muraglia, M.; Carrieri, A.; Bambeke, F. V.; Rosato, A.; Corbo, F. and Franchini, C. 2-aminobenzothiazole derivatives: search for new antifungal agents. *Eur. J. Med. Chem*. **2013**, *64*, 357–364.

4. Ershad, S.; Sagathforoush, L.; Karim-Nezhad, G. and Kangari, S. Electrochemical behavior of N_2SO Schiff-Base Co (II) complexes in non-aqueous media at the surface of solid electrodes. *Int. J. Electrochem. Sci*. **2009**, *4*, 846–854.

5. Singh, D.; Kumar, R. and Singh, J. Synthesis and spectroscopic studies of biologically active compounds derived from oxalyldihydrazide and benzyl, and their Cr(III), Fe(III) and Mn(III) complexes. *Eur. J. Med. Chem*. **2009**, *44*, 1731–1736.

6. Antil, N.; Kumar, M.; Verma, K. K. and Garg, S. Complexes of organyltellurium(IV) with neutral [N,O] donor Schiff Base derived from substituted furfuraldehyde and toluidine: synthesis, structural characterization, computational studies and biological evaluation. *Asian J. Chem.* **2022**, *34*, 1125–1113.

7. Deswal, Y.; Asija, S.; Dubey, A.; Deswal, L.; Kumar, D.; Jindal, D. K. and Devi, J. Instigating the in vitro antidiabetic activity of new tridentate Schiff base ligand appended M(II) complexes: from synthesis, structural characterization, quantum computational calculations to molecular docking, and molecular dynamics simulation. *Appl. Organomet. Chem.* **2023**, *37*, e7050.

8. Gao, K. and Mi, H. Application of membrane-inlet mass spectrometry to measurements of photosynthetic processes. In *Research Methods of Environmental Physiology in Aquatic Sciences,* K. Gao, D. A. Hutchins, J. Beardall, Eds.; Springer: Singapore, **2021**, *11*, 187–192.

9. Musa, A.; Suraj, I.T and Sanusi, S. Synthesis, characterization and antimicrobial studies on Schiff Base derived from 4-amino-2-hydroxybenzoic acid and 2-hyroxybenzaldehyde and its Cobalt (II) and Nickel (II) complexes. *J. Appl. Nat. Sci.* **2022**, *2*, 1–7.

10. Ndifon, P.; Kuate, M.; Ngandung, E.; Paboudam, A. G.; Mariam, C. A.; Peucheu, C. and Tonle, K. I. Cobalt (II), Nickel (II) and Copper (II) complexes of tetradentate Schiff Base ligands derived from 4-nitro-o-phenylenediamine: synthesis, characterization, cyclic voltammetry and biological studies. *Egypt. J. Chem*. **2022**, *65*, 477–495.

11. Abdulmajeed, A.M.; Hanan, A.M. and Sultan, A.H. Short review on metal complexes of Schiff Bases containing antibiotic, and bioactivity applications. *J. Nutr. Biochem*. **2022**, *3*, 1–14

12. Devi, A. G.; Suresh, B. K.; Shridhar, N. M. and Rakesh, R. C. In Vitro antimicrobial activity of cobalt ferrite nanoparticles synthesized by co-precipitation method. *Acta Chem. Iasi*, **2020**, *28*, 225–236.

13. Nassar, D. A.; Ali, O. A. M.; Shehata, M. R. and Sayed, A. S. S. Spectroscopic investigation, thermal behavior, catalytic reduction, biological and computational studies of novel four transition metal

complexes based on 5-methylthiophene Schiff Base type. *Heliyon* **2023**, *9*, e16973.

14. Ribeiro, N.; Farinha, P. F.; Pinho, J. O.; Luiz H.; Mészáros, J. P.; Galvão, A. M.; Pessoa, J. C.; Enyedy, E. A.; Reis, C. P.; Correia, I. and Gaspar, M.M. Metal coordination and biological screening of a Schiff Base derived from 8-hydroxyquinoline and benzothiazole. *Pharmaceutics* **2022**, *14*, 2583.

15. Hanif, M.; Noor, A.; Muhammad, M.; Ullah, F.; Tahir, M.N.; Khan, G.S. and Khan, E. Complexes of 2-amino-3-methylpyridine and 2-amino-4-methylbenzothiazole with Ag(I) and Cu(II). Structure and biological applications. *Inorganics* **2023**, *11(4)*, 152.

16. Witwit, I. N.; Farhan, H. M and Mubark, H. M. Synthesis, chemical characterization, and bacterial inhibition studying of new mixed ligand complexes of 4-Methylimidazoleazo ligand, and ethylenediamine with some divalent metal ions. *Pak. J. Med. Health Sci.* **2022**, *16*, 579–582.

17. Hameed, G. F.; Wadday, F. Y.; Farhan, M. A. A. and Hussain, S. A. Synthesis, spectroscopic characterization and bactericidal valuation of some Metal (II) complexes with new tridentate heterocyclic azo ligand type (NNO) donor. *Egypt. J. Chem.* **2021**, *64*, 1333–1345.

18. Al-Farhan, B. S.; Basha, M. T.; Abdel Rahman, L. H.; El-Saghier, A. M.; El-Ezz, D. A.; Marzouk, A.; Shehata, M. R. and Abdalla, E. M. Synthesis, DFT calculations, antiproliferative, bactericidal activity and molecular docking of novel mixed-ligand Salen/8-hydroxyquinoline metal complexes. *Molecules* **2021**, *26,* 4725.

19. Masoud, M. S.; Ali, A. E.; Abd Elfatah, A. S. and Amer, G. E. Synthesis, molecular spectroscopy, computational, thermal analysis and biological activity of some orotic acid complexes. *Open J. Inorg. Non-Met. Mater*. (*OJINM*) **2021**, *11*, 1–22.

20. Valarmathy, G.; Subbalakshmi, R.; Sumathi, R. and Renganathan, R. Synthesis of Schiff base ligand from n-substituted benzenesulfonamide and its complexes: spectral, thermal, electrochemical behavior, fluorescence quenching, in vitro-biological and in-vitro cytotoxic studies. *J. Mol. Struct.* **2020**, *1199*, 127029.

21. Reena, V. N.; Kumar, K. S.; Bhagyasree, G. S. and Nithyaja, B. One-pot synthesis, characterization, optical studies and biological activities of a novel ultrasonically synthesized Schiff base ligand and its Ni(II) complex. *Results Chem*. **2022**, *4*, 100576.

22. Wadday, F. Y. and Hussein, A. A. Synthesis, identification, thermodynamic and biological studies of new ligand derivative from l-ascorbic acid and its complexes with some metal ions. *Res. J. Pharm. Technol*. **2022**, *15*, 3452–3458.

23. Kumar, B.; Devil, J.; Dubey, A.; Tufail, A. and Taxak, B. Investigation of antituberculosis, antimicrobial, antiinflammatory efficacies of newly synthesized transition metal (II) complexes of hydrazone ligands: structural elucidation and theoretical studies. *Sci. Rep*. **2023**, *13*, 15906.

24. Sánchez-Lara, E.; García-García, A.; González-Vergara, E.; Cepeda, J. and Rodríguez-Diéguez, A. Magneto-structural correlations of cyclo-tetravanadates functionalized with mixed-ligand Copper (II) complexes. *New J. Chem.* **2021**, *45*, 5081–5092.

25. Abu Dief, A. M.; Abdel Rahman, L. H. and Abdel Mawgoud, A. H. A robust in vitro anticancer, antioxidant and antimicrobial agents based on new metal-azomethine chelates incorporating Ag (I), Pd (II) And VO (II) cations: probing the aspects of DNA interaction. *Appl. Organomet. Chem.* **2020**, *34*, 1–20.

26. Devi, J.; Sharma, S.; Kumar, S.; Kumar, B.; Kumar, D.; Jindal, D. K.; Das S. Synthesis, characterization, in vitro antimicrobial and cytotoxic studies of Co(II), Ni(II), Cu(II), and Zn(II) complexes obtained from Schiff base ligands of 1, 2, 3, 4-tetrahydro-naphthalen-1-ylamine. *Appl. Organomet. Chem*. **2022**, *36*, e6760.

27. El-Boraey, H. A.; AboYehia, S. M. and El-Gammal, O. A. Influence of high energy Γ-irradiation on some binuclear transition metal complexes of pentadentate ligand: spectral, thermal, modelling, X-Ray diffraction, morphological and solid electrical conductivity. *Appl. Radiat. Isot*. **2022**, *182*, 110121.

28. Alkhatib, F. M. and Alsulami, M. H. Synthesis, characterization, DFT calculations and biological activity of new Schiff base complexes. *Heliyon* **2023**, *9*, e18988.

29. Xue, L. W.; Zhang, H. J. and Wang, P. P. Synthesis, crystal structures, and antimicrobial activity of copper(II) complexes derived from N′-(1-(pyridin-2-yl)ethylidene)isonicotinohydrazide, *Inorg. Nano-Met.* **2020**, *50*, 637–643.

30. Mutlu Gençkal, H.; Erkisa, M.; Alper, P.; Sahin, S.; Ulukaya, E. and Ari, F. Mixed ligand complexes of Co (II), Ni (II) and Cu (II) with quercetin and diimine ligands: synthesis, characterization, anti-cancer and anti-oxidant activity. *J. Biol. Inorg. Chem.* **2020**, *25*, 161–177.

31. Mahdi, Q. M. and Alias, M.F. Synthesis, characterization, and antimicrobial activity by coordinated metals ions Rh^{+3}, Au^{+3} with sodium fusidate and 2,2-bipyridine as ligands. *Chem. Methodol.* **2022**, *6*, 929–939.